Hindawi
Advances in Materials Science and Engineering
Volume 2019, Article ID 8238904, 16 pages
https://doi.org/10.1155/2019/8238904

Research Article

Development of a Correlation between the Resilient Modulus and CBR Value for Granular Blends Containing Natural Aggregates and RAP/RCA Materials

Muhammad Arshad [1,2]

[1] *Department of Geological Engineering, University of Engineering & Technology, Lahore, Pakistan*
[2] *Department of Civil Engineering, McMaster University, Hamilton, Canada*

Correspondence should be addressed to Muhammad Arshad; arshadm@tcd.ie

Received 4 December 2018; Accepted 14 February 2019; Published 1 April 2019

Academic Editor: Claudio Pettinari

Limited supplies of natural aggregates for highway construction, in addition to increasing processing costs, time, and environmental concerns, have led to the use of various reclaimed/recycled materials. Reclaimed asphalt pavement (RAP) and recycled concrete aggregate (RCA) have prospective uses in substantial amounts in base and subbase layers of flexible pavement in order to overcome the increasing issue of a shortage of natural aggregates. This research presents the development of an empirical model for the estimation of resilient modulus value (M_R) on the basis of CBR values using experimental results obtained for 52 remoulded granular samples containing natural aggregates, RCA, and RAP samples. Statistical analysis of the suggested model shows promising results in terms of its strength and significance when *t*-test was applied. Additionally, experimental results also show that M_R value increases in conjunction with an increase in RAP contents, while the trend for the CBR value is the opposite. Statistical analysis of simulation results using PerRoad and KenPave demonstrates that addition of RAP contents in the subbase layer of flexible pavements significantly improves its performance when considering resistance against rutting and fatigue. However, results of repeated load triaxial tests show that residual accumulative strain under a certain range of loading conditions increases substantially due to the addition of RAP materials, which may be disadvantageous to the serviceable life of the whole pavement structure.

1. Introduction

The highway construction industry is responsible for almost 30% of global air pollution and greenhouse gas emissions and contributes roughly a quarter of the total fossil fuel consumption across the world [1]. Replacing natural or virgin aggregates with high-quality recycled materials has considerable potential to reduce the carbon footprint of the road/pavement construction industry. The overall financial and environmental savings due to the replacement of natural aggregates with recycled materials can rationalise the stabilisation cost in pavement applications. Hence, low-carbon and low-cost substitutes for conventional aggregates are actively being sought by researchers worldwide [2]. Reclaimed asphalt pavement (RAP) [3, 4] and recycled concrete aggregate (RCA) [5–7] have been reported as the most commonly recycled materials used in different layers of flexible pavements, while use of recycled bricks [8], recycled glass [9–11], and fly ash [12] has also been documented by many researchers and institutions.

In general, RAP materials are a blend of coarse and fine aggregates and bitumen obtained from aged or expired asphalt pavements. Throughout the world, major use of RAP material in a surfacing layer is commonly termed as hot mix asphalt (HMA). RAP has been used in the surface layer of flexible pavements in combination with natural aggregates in different percentages, extending up to 80% in some cases [13]. Most of the researchers suggest a typical range of 20–50% [12, 14, 15]. This shows that RAP materials should also be used in base/subbase layers of pavement in addition to using them to make blends with natural granular material in HMA applications. RCA can be obtained from the revamping or demolition of different types of structures, including commercial and residential buildings or other civil engineering structures [16–18]. Many researchers have found that the engineering properties of RCA are either comparable to, or even better than, typical natural aggregates used in road construction [19, 20]. This implies that RCA products have potentially suitable applications in subbase or base course. It should also be noted that RCA can be used as premium base course materials [21].

Conventional pavement design usually depends on the "California bearing ratio" (CBR) of the soil/aggregate used in pavement structure, while the resilient modulus value (M_R) of unbound aggregates is the fundamental input parameter required in the mechanistic empirical design/analysis of pavement structures. The most reliable, and hence most desirable, way to determine the resilient moduli is through repeated triaxial load testing. However, because of the difficulties encountered with the test procedure, including time consumption and the economy of the project, other laboratory tests, such as CBR, would also be considered if a reliable correlation could be established for the estimation of the M_R value. In the existing literature, there are many studies to correlate resilient modulus values to those with CBR values determined for the natural granular materials. However, studies incorporating RAP/RCA instead of natural materials are very limited. Furthermore, a rational or coherent mechanism of the correlation development could probably not be identified, owing to the fact that the mechanics of both of these tests are starkly different from each other.

The specific objectives of this paper are as follows:

(1) To develop a rational model for the prediction of a resilient modulus value of unbound granular materials containing RAP/RCA as a major component on the basis of CBR values;
(2) To evaluate the performance of blended samples used in subbase layers through the computer software packages PerRoad and KenPave;
(3) To evaluate the long-term performance of blended samples under a range of cyclic loading conditions.

Furthermore, a brief literature review on correlations for the estimation of M_R values, with major emphasis on the development of a correlation between CBR value and resilient modulus, is presented in the next section of this research paper.

2. Existing Regression Models for the Prediction of M_R Value

From the existing literature, regression models for the prediction of M_R value for granular material can be categorically divided into four types:

Class I. In this category, the models are based on single strength or stiffness parameter of soil such as

(i) CBR values [22–26];
(ii) *R*-value [27–31];
(iii) Unconfined compressive strength [32];
(iv) Undrained compressive strength [33].

Class II. In this category, the models are based on soil properties and stress state, for instance,

(i) Bulk stress and index properties of the soil [34];
(ii) Unconfined compressive strength and index properties of the soil [35];
(iii) *R*-value and index properties of the soil [36].

Regression models based on this methodology have markedly varying intricacy and acceptability in the research community [32, 37–39].

Class III. In this approach, resilient modulus value for a certain soil is obtained by considering a certain type of stress invariant or set of stress invariants, for instance,

(i) Bulk stress [27];
(ii) Confining pressure and deviator stress [40]; and bulk stress and atmospheric pressure [41];
(iii) Bulk stress, atmospheric pressure, and deviator stress [42];
(iv) Bulk stress, atmospheric pressure, and octahedral shear stress [43];
(v) Atmospheric pressure, octahedral normal stress, and octahedral shear stress [44].

In this category, the model parameters are given simple numerical values.

Class IV. There are also certain constitutive equations for the estimation of resilient modulus values derived from considering soil's physical properties incorporated in model parameters in addition to stress invariant [45–48].

Since this research is focused on the establishment of a correlation between CBR value and resilient modulus value, it is logical to further explain such attempts in a historical perspective.

A number of researchers, including Porter [49, 50], Hight and Stevens [51], and Fleming and Rogers [52] pointed out that the CBR tends to be a bearing value (more of a parameter in terms of strength) rather than a support value (in terms of recoverable behaviour) of materials. Thompson and Robnett [53] could not find a suitable correlation between CBR and M_R; Hight and Stevens [51] stated that the CBR does not correlate consistently with either strength or stiffness; and Sukumaran et al. [54] opined that there is an apparent wide variation in the M_R value that can be obtained using the CBR, which depends on many factors. On the other hand, Lister and Powell [55] felt positive that the CBR can be related, within reasonable limits, to subgrade stiffness. Hossain [56] believed that the CBR test is still one of the most widely used tests for evaluating the competency of pavement subgrade; however, there are variations in the procedure followed by different agencies (e.g., in terms of size of mould, compaction techniques, and efforts), and it was found that [56] correlations between resilient modulus values and all test results (including the CBR) were not statistically significant. Garg et al. [57] opined that the CBR value can be converted to a resilient modulus; a strong trend is apparent in the correlation but there is a lot of scatter. A few of the existing correlations based on CBR values are given in Table 1.

Table 1: Existing models for the estimation of resilient modulus based on CBR value.

$M_R = 10.33\text{CBR}$	[23]
$M_R = 38\,(\text{CBR})^{0.711}$	[22]
$M_R = 18\,(\text{CBR})^{0.64}$	[55]
$M_R = 21\,(\text{CBR})^{0.65}$	[58]
$M_R = 17.6\,(\text{CBR})^{0.64}$	[59]

3. Material Characterisation

For this research, four different types of RAP samples (designated as "RAP(1)," "RAP(2)," "RAP(3)," and "RAP(4)"), three different types of natural aggregates (designated as "*A*," "*F*," and "*W*"), and one RCA sample were used. Based on the gradation curves, natural aggregate *A* is finer than other natural aggregate (*F* and *W*) while natural aggregate *W* is the most coarser among them. Each of the natural aggregate samples, as well as the RAP and RCA materials, contained crushed limestone of subangular to angular shape. Elongated and flat particles in the samples/materials were not more than 6% as per ASTM D 4791.

A summary of material characterisations in terms of detailed gradation properties ($D_{10}/D_{30}/D_{50}$ grain size diameter corresponding to 10/30/50 percent finer by mass; C_c coefficient of curvature; C_u coefficient of uniformity), compaction characteristics, effective shear strength parameters, and physical properties of recovered bitumen binders has been presented in Table 2. Further detail on material characterisation can be found in Arshad and Ahmed [60] and Arshad [61]. Since focus of the testing campaign consists of the CBR test and the resilient modulus test, the same has been briefly explained in the following subsections.

Table 3 shows the matrix of the testing program including the resilient modulus tests, the CBR tests, and the repeated load tests.

3.1. CBR Test. In conventional pavement design, the CBR value is an important parameter used to determine the thickness of various layers of the pavement structure. Usually, the higher the CBR value, the better the performance of the pavement is, with regard to both stiffness and strength. This implies that the CBR value can be used as a parameter to evaluate the suitability of a soil for use as pavement construction material. For this study, standard 3-point CBR tests were performed on the natural/RAPs and blended samples under unsoaked conditions, to simulate the moisture content at which the resilient modulus tests were performed. A schematic diagram of the CBR test is shown in Figure 1.

The test equipment primarily consisted of a:

(1) cylindrical mould having an inner diameter of 150 mm and a height of 175 mm;

(2) spacer disc of 148 mm in diameter and 47.7 mm in height;

(3) special surcharge weights;

(4) metallic penetration piston of 50 mm diameter and minimum of 100 mm in length;

(5) loading machine with a capacity of at least 50 kN and equipped with a movable head or base that travels at a uniform rate of 1.25 mm/min.

The CBR value is defined as the ratio of stress required for the circular piston to penetrate, at the rate of 1.25 mm/min, the soil mass in the cylinder to the standard stress that is required for the corresponding penetration of a standard material, i.e., like limestone found in California. Further procedural details on the CBR value calculations can be found in AASHTO T 193.

3.2. Resilient Modulus Test. Resilient modulus (M_R) is defined as the ratio of cyclic axial stress to recoverable axial strain ($\Delta\sigma_c/\Delta\varepsilon_a$). The cylindrical test specimen is compacted at a desired density and is subjected to cyclic axial stress at a given confining pressure within a conventional triaxial cell. Resilient modulus tests for this research were conducted as per the guidelines specified in AASHTO T 307-99(2004), for which a haversine-shaped loading waveform is mandatory to simulate traffic loading. Each load cycle of this waveform essentially consists of 0.1 seconds load duration and a 0.9 second rest period. Figure 2 shows a typical repetitive load/stress pulse along with the generated residual deformation curve in the time domain. The regular loading sequence in AASHTO T 307-99 consists of 15 different stages, each one having 100 load cycles, following the execution of the conditioning stage of 750 load cycles. Each of the loading stages has a particular combination of confining stress, maximum axial stress, and cyclic deviator stress as shown in Table 4. Further procedural details of the test including sample preparation and installation technique; electromechanics of the loading system (servo-controlled electrohydraulic MTS testing machine); specification of the used load cells and LVDTs; and particulars of the data acquisition system can be found in several works [60–62].

4. Test Results and Discussion

This section presents a discussion on trends obtained for the CBR tests and the resilient modulus tests performed on a number of reconstituted granular samples as identified in Table 2.

4.1. Sample Results of the CBR Test. Sample results of the CBR test in terms of compaction effort and the percentage of RAP content on the CBR values are presented in Figure 3. From this figure, it can be inferred that the CBR value decreases

Table 2: Characterisation of the tested materials.

Material	Compaction characteristics (AASHTO T180)						
	Maximum dry density (kN/m^3)			Optimum moisture content (%)			
Natural aggregates	21.9–23.3			5.5–7.1			
RAPs	19.7–21.4			6.4–9.1			
RCA	20.7			7.5			
	Gradation characteristics (AASHTO T27-99)						
	D_{10} (mm)	D_{30} (mm)	D_{50} (mm)	Cu	C_c	% Sand size (mm)	% (4.75–9.5) mm
Natural aggregate *A*	0.15	0.45	1	11.7	0.77	70	10
Natural aggregate *F*	0.15	1.5	9	100.0	1.00	35	10
Natural aggregate *W*	0.6	5	15	33.3	2.08	25	12
RAP(1)	0.3	1.2	2.75	13.3	1.20	64	22
RAP(2)	0.3	1.2	2.75	13.3	1.20	60	30
RAP(3)	1.5	5	6.5	5.0	2.22	27	50
RAP(4)	0.3	1.2	2	9.2	1.75	82	10
RCA	0.25	1.5	6.5	40.0	0.9	40	18
	Flat and elongated particles (ASTM D 4791)						
Natural aggregates/RAPs/RCA	Limited to 6%						
	Shear strength parameters under quick shear test						
Natural aggregates/RAPs/RCA	Friction angle			Cohesion			
	36°–43°			20–30 kPa			
	Physical properties of recovered bitumen binder						
RAPs	60°C viscosity (poise) (ASTM D4402)	25°C penetration (dmm) (ASTM D5-06)		Softening point (°C) (ASTM D36-76)			
	23500–46700	20–52		62–67			

Table 3: Matrix of the testing program.

Natural aggregate/RCA	RAP	Minimum number of resilient modulus tests	Minimum number of CBR tests	Minimum number of repeated load triaxial tests
Natural aggregate *A*, *F*, *W*	—	3	3	2
RCA	—	1	1	—
Blends of natural aggregates with RAPs	$4 \times 3^*$	$3 \times 3 \times 4 = 36$	$3 \times 3 \times 4 = 36$	7
Blends of RCA with RAPs	$4 \times 3^*$	$3 \times 4 = 12$	$3 \times 4 = 12$	—
Total		52	52	9

*Blended samples were prepared by mixing 25%, 50%, and 75% (by weight) of each RAP type with the natural aggregates and RCA.

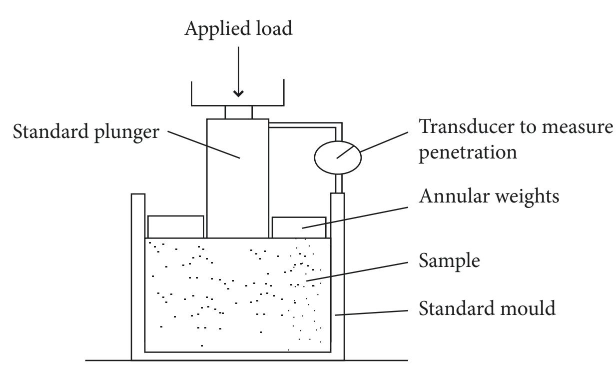

Figure 1: A schematic diagram of the CBR test.

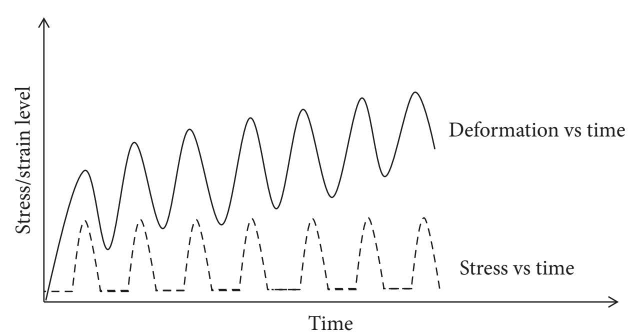

Figure 2: Typical shape of applied repeated load cycles and the generated deformation curve.

noticeably in correspondence to the increasing content in the blended samples incorporating granular (A) and RAP(1). For instance, the blend containing 25% RAP(1) achieves only 74% of the CBR value achieved by the aggregate (*A*) (natural material) at the same level of compaction effort, i.e., 65 blows. Similarly, the corresponding value for blends containing 50% RAP(1), 75% RAP(1), and 100% RAP(1) is limited to 56.25%, 32.5%, and 22.5%, respectively. Likewise, the trend can also be observed for the other two compaction efforts consisting of 10 and 30 blows.

4.2. Effect of RAP Contents on Resilient Modulus (M_R). Forty-eight blended samples were prepared by mixing the four types of RAP materials with natural granular samples *A*, *F*, *W*, and RCA in proportion with RAP contents of 25%,

Table 4: Loading sequence for the resilient modulus test as per AASHTO T 307 protocol.

Seq. No.	No. of load applied	Confining stress σ_3 (kPa)	Max. axial stress σ_{max} (kPa)	Cyclic axial stress σ_{cyclic} (kPa)	Contact stress $0.1\sigma_{max}$ (kPa)	Total axial stress (kPa)
0	750	103.4	103.4	93.1	10.3	206.8
1	100	20.7	20.7	18.6	2.1	41.4
2	100	20.7	41.4	37.3	4.1	62.1
3	100	20.7	62.1	55.9	6.2	82.8
4	100	34.5	34.5	31	3.5	69
5	100	34.5	68.9	62	6.9	103.4
6	100	34.5	103.4	93.1	10.3	137.9
7	100	68.9	68.9	62	6.9	137.8
8	100	68.9	137.9	124.1	13.8	206.8
9	100	68.9	206.8	186.1	20.7	275.7
10	100	103.4	68.9	62	6.9	172.3
11	100	103.4	103.4	93.1	10.3	206.8
12	100	103.4	206.8	186.1	20.7	310.2
13	100	137.9	103.4	93.1	10.3	241.3
14	100	137.9	137.9	124.1	13.8	275.8
15	100	137.9	275.8	248.2	27.6	413.7

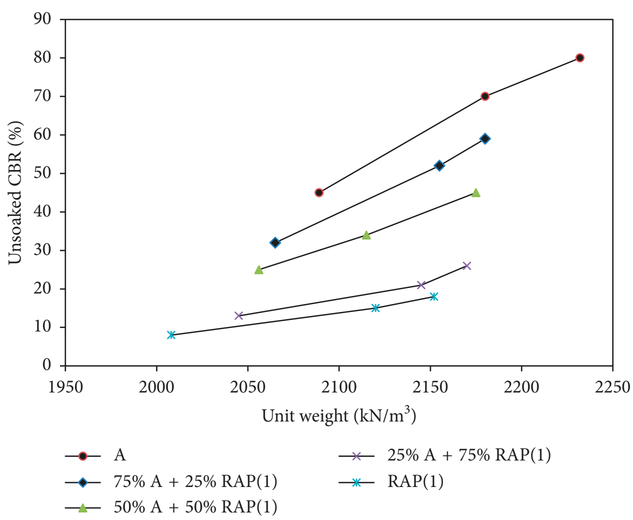

Figure 3: Effect of RAP contents on CBR values.

50%, and 75% for each. Figures 4(a)–4(d) show the effects of the addition of these RAPs on the measured M_R values over a range of bulk stresses as specified in AASHTO T 307-99 (68). Variation of M_R values with bulk stress can be approximated through trend lines based on a power function having the coefficient of determination (R^2) in the range of 0.95–0.99. From these trend lines, it is evident that M_R values increase not only due to the increase in bulk stress but also in combination with the addition of RAP contents, i.e., blended samples give higher M_R values when compared to those obtained from the natural samples of granular *A*, *F*, *W*, and RCA. More specifically, for instance, at a bulk stress of ~673 kPa, M_R value for the 100% granular *W* is 320 MPa while the corresponding values for blended samples incorporating 25%, 50%, and 75% of RAP(1) are 340 MPa, 360 MPa, and 390 MPa, respectively.

A similar trend in M_R values was observed at lower levels of bulk stress, or more precisely, over the entire range of bulk stresses considered during the testing campaign. In some cases, ~50% increase in M_R values was observed for the blends containing 75% RAP contents. In general, for most of the blended samples containing 25% and 50% RAP contents, the corresponding increase in M_R values was in the range of 5–15% and 10–20%, respectively. An important point is that the addition of RAPs to RCA induced the most significant increase in the resilient moduli when compared with the increase in M_R when RAP was added to granular samples. Similar observations have also been documented by many researchers, including Kim and Labuz [12], MacGregor et al. [63], Alam et al. [64], and Bennert and Maher [65].

5. Development of Correlation between Resilient Modulus and CBR Values

5.1. Proposed Correlation and Theoretical Background. For this study, an attempt has been made to correlate the M_R values with the CBR values on the basis of a common value of bulk stress identified during both types of tests. This should be emphasize that CBR values tend to decrease with addition of RAP contents while reverse is the situation in case of resilient modulus values. Such trends are primarily due to the fact that loading for the resilient modulus test is dynamic in nature while in the case of the CBR test, it is virtually static.

Fundamentally, axial stress is applied during the CBR tests through a plunger (σ_{pa}) in addition to an axial surcharge weight (σ_{sa}) as shown in Figure 5. However, lateral stress on the walls of the CBR mould can be estimated on the basis of the lateral earth pressure coefficient (K_a) as described in classical soil mechanics, such that

$$\begin{aligned} \sigma_{pl} &= K_a \sigma_{pa}, \\ \sigma_{sl} &= K_a \sigma_{sa}, \\ K_a &= 1 - \sin(\phi), \end{aligned} \tag{1}$$

where ϕ is the effective angle of internal friction of the soil sample (blend) under consideration.

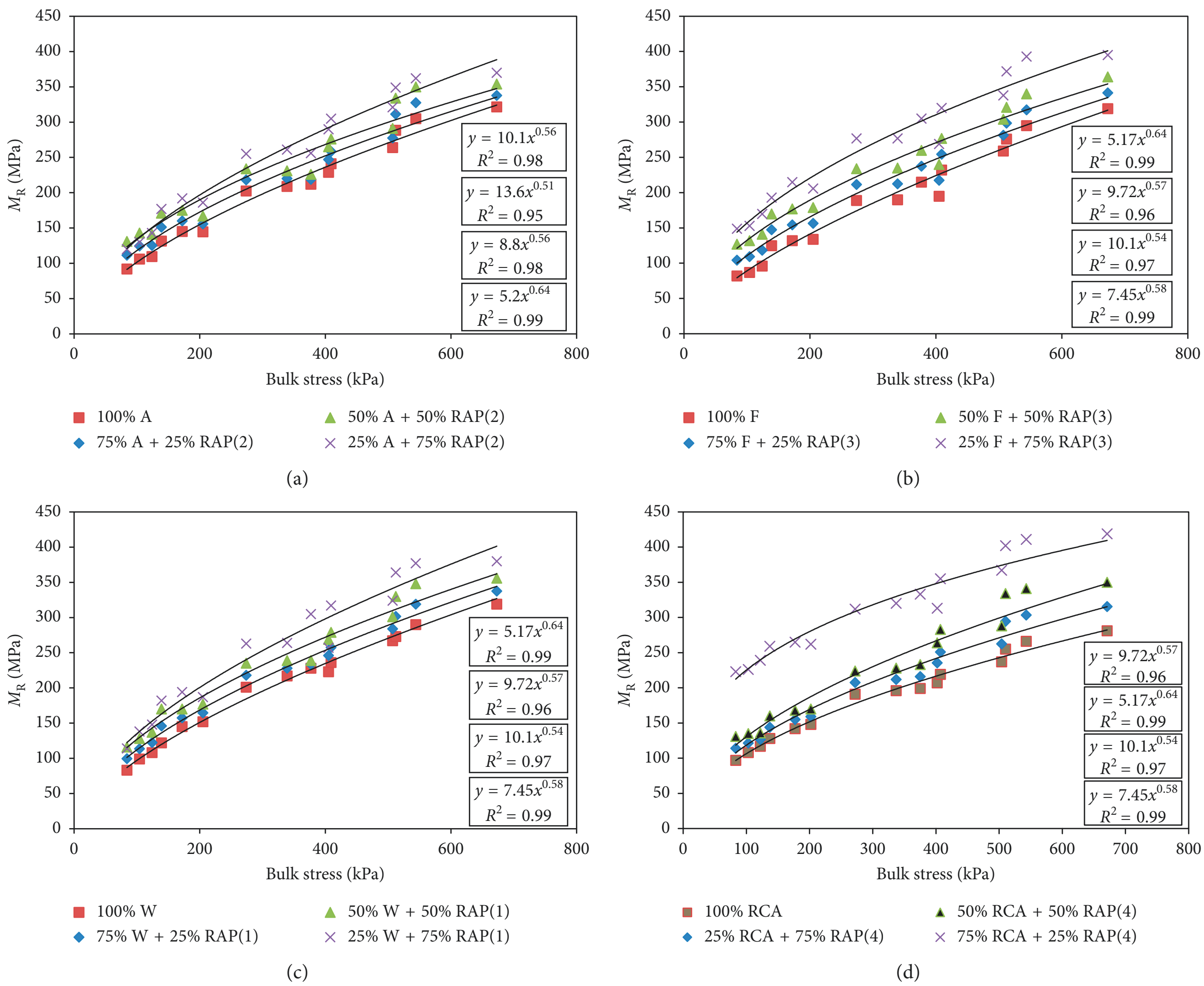

FIGURE 4: Variation of M_R value with bulk stress and percentage of RAP contents for (a) natural *A*; (b) natural *F*; (c) natural *W*, and (d) RCA.

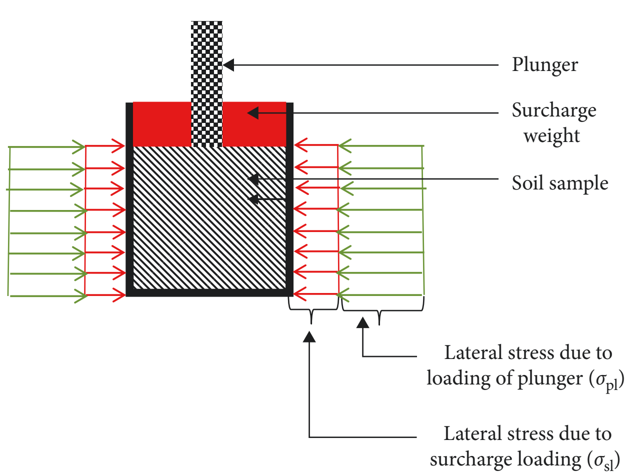

FIGURE 5: An assumed configuration of axial and lateral stresses during CBR test.

It is interesting to note that the 3-point CBR test encompasses a wide range of dry and bulk density in the sample, while on the other hand, each resilient modulus test uses a unique value of the sample's dry and bulk density. To estimate a unique value of the bulk stress during the CBR test which is analogous to the bulk stress value identified from resilient modulus test, the following procedure was adopted:

(1) Determine the dry density of the resilient modulus sample

(2) Estimate the CBR value corresponding to that dry density value

(3) Determine the axial stress (σ_{pa}) value corresponding to the CBR value

(4) Calculate the bulk stress using the following relation:

$$\sigma_{bulk} = \theta = \sigma_1 + \sigma_2 + \sigma_3 = \left(\sigma_{pa} + \sigma_{sa}\right) + 2K_a\left(\sigma_{pa} + \sigma_{sa}\right). \quad (2)$$

Using a unique value of bulk stress on the basis of equation (2), the corresponding resilient modulus value from the actual experimental data (M_R test) was matched and then a correlation between CBR value (point 2) and the resilient modulus value, in terms of the power function having a coefficient of determination ~0.81, can be given as

$$M_R = 49.37\,(\mathrm{CBR})^{0.59}. \tag{3}$$

Table 5 shows the experimental data and the estimated values of M_R based on the four steps explained above and equation (3).

Figure 6 shows the capabilities of the proposed regression model on the basis of the distribution of the data points, which in fact involves the experimentally determined and estimated M_R values along the unity line, giving a 95% prediction and confidence interval. This figure illustrates that there is an almost equal distribution of the data points on both sides of the unity line. Additionally, the entire set of the data points is confined within the 95% prediction interval, which is defined as the interval around the linear regression line such that 95% of the predicted values will fall in this interval. Further details on the mathematical framework of the prediction and the confidence interval can be found in standard textbooks dealing with statistics and probability analysis, such as those authored by Wonnacott and Ronald [66], Penny and Roberts [67], and Dybowski and Roberts [68].

5.2. Statistical Analysis of the Proposed Model. A Pearson's correlation coefficient (r), as given by equation (4), is a measure of the strength and direction of linear association that exists between two continuous variables. More specifically, for the drawn line of best fit for sample data points of two variables, Pearson's correlation indicates how well the data points fit this new model/line of best fit, and its numerical value indicates how far away all these data points are to the line of best fit (i.e., how well the data points fit this new model/line of best fit) [69, 70]:

$$r = \frac{\sum_{i=1}^{n}\left(u_i - \overline{u}_i\right)\left(t_i - \overline{t}_i\right)}{\sqrt{\sum_{i=1}^{n}\left[\left(u_i - \overline{u}_i\right)^2\left(t_i - \overline{t}_i\right)^2\right]}}, \tag{4}$$

where u_i and t_i = experimental and predicted values, respectively, for the ith output, $\overline{u}_i$ = average of experimental outputs, and n = size of sample.

The statistical value of r may range from −1 for a perfect negative linear relationship (inversely related) to +1 for a perfect positive linear relationship (directly related). In general, from theoretical point of view, the strength of the linear relationship can be categorised as "very strong," "moderately strong," and "fairly strong" for the corresponding numerical values of r in the range 0.8–1.0, 0.6–0.8, and 0.3–0.5 [71]. It should be emphasized that if $r = 0.0$ it does not necessarily mean that the two variables have no relationship. In order to look into the real strength of the correlation, usually, a statistical test of significance is performed, as discussed in [72]. For this study, three different types of statistical tests were applied to assess the significance of the developed correlation presented in equation (3) and Table 5.

Case 1. t-Test for the assessment of the implication of coefficient of correlation (r) at a specific degree of freedom and level of significance [73].

This provides the researcher with some idea of how large a correlation coefficient must be before it can be considered as demonstrating that there really is a relationship between two variables (in our case the $(M_R)_{\text{measured}}$ and CBR values). It may be the situation that two variables are related by chance, and a hypothesis test for r allows the researcher to decide whether the observed r could have emerged by chance or not. The null hypothesis is that there is no relationship between the two variables. That is, if ρ is the true correlation coefficient for the two variables and when all population values have been observed, then the null hypothesis can be given as

$$H_0\colon\ \rho = 0. \tag{5}$$

The alternative hypothesis could be written as

$$H_A\colon\ \rho \neq 0, \tag{6}$$

whereas the standardised t-test for the null hypothesis that r is equal to zero can be written as

$$t = r\sqrt{\frac{n-2}{1-r^2}}, \tag{7}$$

where n is the number of paired observations in the given sample.

The null hypothesis is evaluated by comparing the *t-statistic* of equation (7) with *t-critical* (2.01) obtained from *t distribution* having the $n-2$ degree of freedom.

Case 2. Direct comparison of the coefficient of correlation value (0.9) with the *r-critical* value (0.27) obtained from a statistical table corresponding to a specific degree of freedom and level of significance [61, 74].

Case 3. It often becomes mandatory to statistically evaluate the difference between two datasets obtained by two different sources. As in our case, one set of M_R values was obtained experimentally using the AASHTO T 307-99(2004) protocol and the other set of M_R values was obtained using the proposed correlation. A standard t-test was performed to evaluate the difference between the paired values of $(M_R)_{\text{measured}}$ and $(M_R)_{\text{estimated}}$ at a specific degree of freedom and level of significance [74, 75].

Table 6 summarises the statistical analysis of the above three cases.

6. Assessment of Pavement Performance Containing RAP Content in Its Subbase Layer

To examine the performance of the pavement containing natural aggregates mixed with RAP and used as subbase materials, the following analyses were performed using computer software simulation:

(1) To access the likelihood that critical pavement responses exceed predefined thresholds using computer program PerRoad [76];

Table 5: A comparison of measured and estimated M_R values along with CBR values.

Material/Blend	Dry unit weight achieved (kN/m^3)	CBR (%)	Total axial stress (kPa)	Estimated bulk stress in CBR test (kPa)	M_R values measured/projected (MPa)	M_R values estimated (MPa)
100% A	21.1	65	978.0	1663	550	584
100% F	22.1	74	1113.0	1892	600	631
100% W	22.4	85	1278.0	2173	670	685
100% RCA	19.2	53	798.0	1357	410	518
75% A + 25% RAP(1)	20.7	47	708.0	1204	470	482
50% A + 50% RAP(1)	20.5	31	468.0	796	300	377
25% A + 75% RAP(1)	20.2	22	333.0	566	280	308
75% A + 25% RAP(2)	20.3	55	828.0	1408	505	529
50% A + 50% RAP(2)	20.8	39	588.0	1000	410	432
25% A + 75% RAP(2)	21.3	17	258.0	439	260	264
75% A + 25% RAP(3)	20.1	51	768.0	1306	490	506
50% A + 50% RAP(3)	20.5	30	453.0	770	315	370
25% A + 75% RAP(3)	19.9	19	288.0	490	310	282
75% A + 25% RAP(4)	19.7	55	828.0	1408	505	529
50% A + 50% RAP(4)	19.8	43	648.0	1102	402	458
25% A + 75% RAP(4)	19.2	27	408.0	694	252	347
75% F + 25% RAP(1)	20.8	52	783.0	1331	538	512
50% F + 50% RAP(1)	21.3	41	618.0	1051	455	445
25% F + 75% RAP(1)	20.1	14	213.0	362	356	235
75% F + 25% RAP(2)	20.5	59	888.0	1510	525	552
50% F + 50% RAP(2)	19.9	48	723.0	1229	407	488
25% F + 75% RAP(2)	19.7	31	468.0	796	408	377
75% F + 25% RAP(3)	20.1	62	933.0	1586	667	568
50% F + 50% RAP(3)	19.2	41	618.0	1051	516	445
25% F + 75% RAP(3)	20.8	19	288.0	490	343	282
75% F + 25% RAP(4)	21.3	43	648.0	1102	515	458
50% F + 50% RAP(4)	20.1	32	483.0	821	490	384
25% F + 75% RAP(4)	21.3	13	198.0	337	278	225
75% W + 25% RAP(1)	20.8	51	768.0	1306	510	506
50% W + 50% RAP(1)	20.5	44	663.0	1127	500	464
25% W + 75% RAP(1)	19.9	16	243.0	413	240	255
75% W + 25% RAP(2)	19.7	55	828.0	1408	502	529
50% W + 50% RAP(2)	19.9	31	468.0	796	438	377
25% W + 75% RAP(2)	21.3	12	183.0	311	265	215
75% W + 25% RAP(3)	20.1	48	723.0	1229	520	488
50% W + 50% RAP(3)	21.3	35	528.0	898	447	405
25% W + 75% RAP(3)	20.7	21	318.0	541	255	299
75% W + 25% RAP(4)	20.5	45	678.0	1153	480	470
50% W + 50% RAP(4)	19.9	34	513.0	872	473	398
25% W + 75% RAP(4)	19.2	9	138.0	235	213	181
75% RCA + 25% RAP(1)	20.8	38	573.0	974	486	425
50% RCA + 50% RAP(1)	21.3	23	348.0	592	330	316
25% RCA + 75% RAP(1)	20.1	12	183.0	311	187	215
75% RCA + 25% RAP(2)	21.3	38	573.0	974	525	425
50% RCA + 50% RAP(2)	20.1	31	468.0	796	356	377
25% RCA + 75% RAP(2)	21.4	14	213.0	362	200	235
75% RCA + 25% RAP(3)	20.1	32	483.0	821	447	384
50% RCA + 50% RAP(3)	20.5	15	228.0	388	226	245
25% RCA + 75% RAP(3)	19.9	9	138.0	235	148	181
75% RCA + 25% RAP(4)	19.2	39	588.0	1000	473	432
50% RCA + 50% RAP(4)	20.1	13	198.0	337	200	225
25% RCA + 75% RAP(4)	20.2	18	273.0	464	161	273

(2) To determine the stresses and strains at critical locations in the pavement structure using computer program KenPave developed by the University of Kentucky [77].

PerRoad is a Monte Carlo-based simulation software used to develop probability-based analysis for flexible pavement. This software can easily demonstrate the influence of the M_R values of the pavement material on the

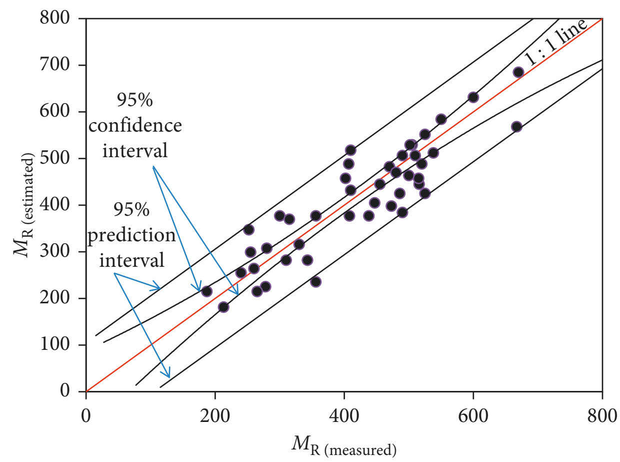

Figure 6: A comparison of estimated and measured M_R values along the unity line.

Table 6: Summary of the statistical analysis of the proposed model at an alpha value of 0.05 which matches to 95% confidence level.

Case			Comments
1	t-Critical = 2.0	t-Statistic = 14.59	Since *t-statistic* > *t-critical* which implies that value of the correlation coefficient is not due to sampling error, the null hypothesis is rejected and it is concluded that there is a significant correlation between $(M_R)_{measured}$ and CBR value in the population.
2	r-Pearson = 0.9	r-Critical = 0.27	Since r-Pearson > *r-critical* which implies that the null hypothesis is rejected, it is quite realistic to accept the "alternative hypothesis," that is the value of r that we have obtained from our sample represents a real relationship between $(M_R)_{measured}$ and CBR value in the population.
3	t-Critical = 2.0	t-Statistic = 0.52	Since *t-statistic* < *t-critical* which implies that the null hypothesis is accepted, it is concluded that there is an insignificant difference between $(M_R)_{measured}$ and $(M_R)_{correlated}$ values in the population.

cumulative damage factor (CDF). It also demonstrates the likelihood that critical pavement responses could exceed predefined thresholds, which are the horizontal tensile strain of 70 microns at the bottom of the asphalt concrete (which is linked with fatigue cracking) and the vertical compressive strain of 200 microns at the top of the subgrade (which is associated with the structural rutting) [78].

6.1. Pavement Structure and Material Characteristics. Figure 7 shows a typical cross section of flexible pavements, which consists of a hot mix asphalt layer supported by the unbound base, unbound subbase, and compacted subgrade. The thickness of each layer generally depends on the traffic load or more specifically, the equivalent single axle load (ESAL) during the proposed life cycle of the road.

In this parametric study, the focus is placed on how the properties of granular subbase materials are changed by the addition of a certain amount of RAP and their effect on the pavement's performance. As such, the resilient modulus of the granular base and the asphalt concrete is fixed. The structure of the pavement to be simulated and the properties of materials in different layers are summarised in Table 7. In this particular study, the subbase material will be one of the aggregates or aggregate/RAP blends tested during the experimental studies of this research.

The properties of the different pavement layers used in the analysis are shown in Table 7. The bulk stresses at the top and bottom of the granular subbase layer were determined using the computer program KenPave. For the selected HMA resilient moduli (M_R = 5000 MPa), the bulk stresses were found in the range of 27 kPa to 30 kPa and 14 kPa to 18 kPa at the top and bottom of the subbase layers, respectively, for the wheel load of 40 kN. In the simulations, values of M_R are used corresponding to the bulk stress of 100 kPa.

6.2. Traffic Load. For this parametric study, the traffic data for urban interstate highways, as recommended by AASHTO, were used. In the case of the PerRoad software, traffic is separated by axle type: single axle, tandem axle, tridem axle, and steer axle. After determining the percentage of each axle type in the total traffic, traffic is then subdivided into weight classes in 2 kip intervals. The following is the summary of the traffic data: the average annual daily traffic (AADT) is 1000 vehicles with 10% being trucks; annual growth rate of traffic is 4%; the directional distribution is 50%; and the percentages of single, tandem, and tridem axles are 55.73%, 42.66%, and 1.61%, respectively. The rest of the traffic loading characteristics, in terms of the distribution of vehicle types and axle weights, are described in Figure 8. These values were used as input in PerRoad 3.5. Axle weights were used to evaluate the response of the pavement layers in terms of stresses, strains, and deformations at critical locations of certain layers of the flexible pavement.

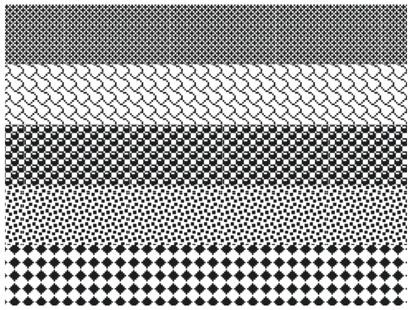

Figure 7: A typical cross section of flexible pavement.

Table 7: Material properties and pavement layer thicknesses.

Parameters	HMA	Base course	Subbase course	Subgrade
M_R (MPa)	5000	350	Variable	35
Coefficient of variation for M_R (%)	25	30	35	45
Thickness of the layer (mm)	250	200	300	—
Thickness Variability (%)	5	8	15	—
Poisson ratio	0.3	0.3	0.3	0.4

6.3. Pavement Performance Criteria. In the design of conventional flexible pavements, pavement sections are designed corresponding to a cumulative damage factor (CDF) of 1.0, which corresponds to a terminal level of pavement damage. For perpetual pavements, however, it is recommended that the CDF is equal to 0.1 at the end of its design life [76]. The fatigue and rutting algorithms developed at Mn/ROAD [79] for the calibration of flexible pavement performance equations were used to predict pavement damage in cases where pavement responses exceeded these thresholds. These correlations are as follows:

$$N_{\mathrm{f}} = 2.83 * 10^{-6}\left(\frac{1}{\varepsilon_t}\right)^{3.148} \quad \text{(fatigue)},$$
$$N_{\mathrm{r}} = 6.026 * 10^{-8}\left(\frac{1}{\varepsilon_v}\right)^{3.87} \quad \text{(ritting)}, \tag{8}$$

where N_{f} = number of load repetitions when fatigue failure occurs, N_{r} = number of load repetition when rutting failure occurs, ε_t = the horizontal tensile strain at the bottom of the HMA, and ε_v = the vertical compressive strain at the top of the subgrade.

It should be noted that the damage of rutting estimated by PerRoad only takes into account the permanent deformation in the subgrade. Any rutting associated with the deformation of granular subbase materials is not considered. According to the test results in this study, use of RAP in granular subbase layers may induce substantial residual deformation. Further investigation should be performed to get a better understanding of its influence on the rutting of flexible pavements.

6.4. Simulation Results and Discussion. Simulation results are obtained and discussed in terms of

(1) The likelihood of the tensile strain at the bottom of the HMA exceeding 70 $\mu\varepsilon$;

(2) The likelihood of the vertical strain at the top of the subgrade soil exceeding 200 $\mu\varepsilon$;

(3) The number of years it could take to reach a CDF of 0.1 (the threshold level) for fatigue damage;

(4) The number of years it could take to reach a CDF of 0.1 for damage induced by rutting.

Figure 9 illustrates the concept frequency distribution for strain both within and outside the threshold limits.

We first examine the likelihood of critical pavement responses exceeding the predefined thresholds when the resilient modulus of the asphalt concrete is 5000 MPa, and different aggregates or aggregate-RAP blends are used in the granular subbase layer. Figure 10 summarises (1) the likelihood of the tensile strain at the bottom of the HMA remaining within the critical value of 70 $\mu\varepsilon$ and (2) the likelihood of the vertical strain at the top of the subgrade soil exceeding 200 $\mu\varepsilon$. From this figure, it can be interpreted that all of the blends result in better pavement performance than the natural aggregate both in terms of the tensile strains at the bottom of the HMA and the vertical compressive strains at the top of the subgrade soil. For instance, the natural aggregates and RCA on average have an 81.3% likelihood that horizontal strain at the bottom of the HMA will remain within the critical limit of 70 $\mu\varepsilon$.

On the other hand, the likelihood for blended materials containing 25%, 50%, and 75% of RAP materials in the blended samples may reach (on average) 85.75%, 89.37%, and 93.77% (respectively) chance of remaining within the limit. Similarly, the likelihood that the compressive strain at the top of the subgrade will not exceed the critical value of 200 microns is 88.28% (natural samples), 93.46% (25% RAP material blends), 95.57% (50% RAP material blends), and 98.2% (75% RAP material blends).

Figure 11 shows the number of years required to reach a CDF of 0.1 when fatigue is controlled by the horizontal tensile strain at the bottom of the subgrade, and the HMA and vertical structural rutting are controlled by the vertical compressive strain at the top of the subgrade. The number of years required to reach a CDF of 0.1, in general, increases in line with the increase in the quantity of RAP in the blend. For example, the number of years required to reach a CDF of 0.1 in terms of fatigue damage at the bottom of HMA is 40.33 years for natural samples, while the corresponding figure for the blends containing 75% RAP is 51.68 years on average. A similar trend regarding an increase in the number of years required to reach a CDF of 0.1 in terms of structural damage at the top of the subgrade was also observed. Furthermore, for all the cases, the number of years to reach a CDF of 0.1 was more than 40 years, but it is clear that fatigue will be the predominant pavement failure mode.

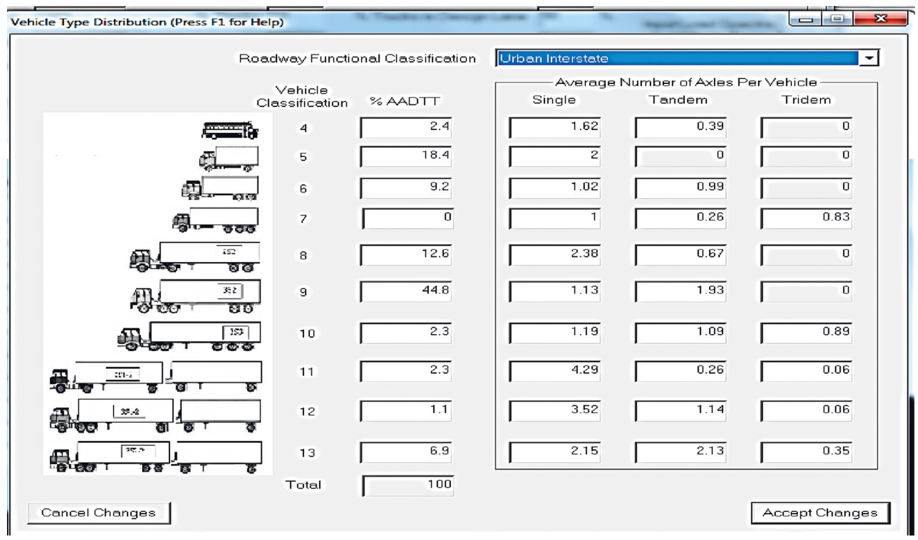

Figure 8: Vehicular load classification used in PerRoad 3.5.

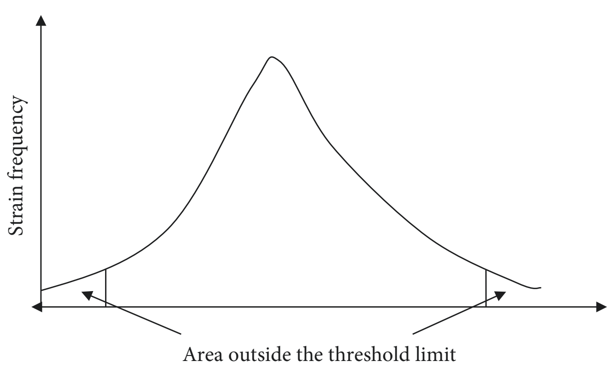

Figure 9: Example of frequency distribution of strain within and outside the threshold limits.

7. Long-Term Effect of Cyclic Loading on Blended Samples

In order to explore the long-term effects of cyclic loading, 9 repeated load triaxial tests were performed under a range of cyclic loading conditions and varying percentages of RAP contents. Figure 12 presents the variation of the residual strain of the tested samples subjected to 20000 load cycles under two different values of confining pressures of 34.5 kPa and 137.9 kPa each, while the corresponding cyclic deviator stress was maintained at 31.05 kPa and 372 kPa. From this figure, it can be inferred that the presence of RAP contents increases the residual strain considerably for both of the confining pressure scenarios. For instance, for the repeated load test conducted at the confining pressure of 34.5 kPa, the residual strain for 100% natural aggregate *F* is 0.12% after 20000 load cycles, while for the blend containing 50% RAP(2) and 75% RAP(2), the corresponding figures reach 0.22% and 0.60%, i.e., an addition of 50% RAP increases the residual strain by a margin of almost 83% while the addition of 75% RAP increases the residual strain by almost 400%. Similarly, for the repeated load tests conducted at a confining pressure of 137.9 kPa on samples containing natural aggregate *W* and the blends with RAP(1) at 50% and 75%, the residual strain after 20000 load cycles is 55% and 300% higher when compared with the corresponding value for the 100% natural aggregate *W*. Furthermore, it is evident from the figures that almost 60% of the total residual strain occurred during the first 2000 load cycles out of the 20000 total load cycles applied across all the cases.

However, it should be emphasized that there is a tendency for the elastic shakedown to be less pronounced for blended samples when compared to pure natural aggregates. For instance, for the blended sample 50% *W* and 50% RAP(1), the rate of increase of strain becomes 0.000154% for the load cycles in the range of 2000–20000. On the other hand, this figure remained limited to 0.000056% for the sample containing 100% natural aggregate *W* under the same loading condition.

Figure 13 shows the effect of the ratio of "*cyclic deviator stress to the confining stress* (σ_d/σ_c)" on the residual strain for the blended sample containing 50% *A* and 50% RAP(3). From this figure, it can be inferred that the ratio σ_d/σ_c has a substantial effect on the residual strain generated under cyclic loading. For instance, at $(\sigma_d/\sigma_c) = 0.9$, the residual strain after 6000 load cycles is limited to 0.06%; however, this value reaches 0.11% and 0.21% at $(\sigma_d/\sigma_c) = 1.8$ and $(\sigma_d/\sigma_c) = 2.7$, respectively. The samples tend to stabilise more quickly under a lower value of $(\sigma_d/\sigma_c) = 0.9$ when compared to the stabilising tendency at the higher values of $(\sigma_d/\sigma_c) = 1.8$ and $(\sigma_d/\sigma_c) = 2.7$, which were also investigated in this research. A 50–60% residual strain occurs during the first 1000 load cycles out of the total 6000 load cycles applied during the experimental campaign, irrespective of the σ_d/σ_c value.

8. Summary and Conclusions

(1) The blended samples (i.e., RAP combined with natural granular materials) result in higher M_R values than those obtained for natural granular

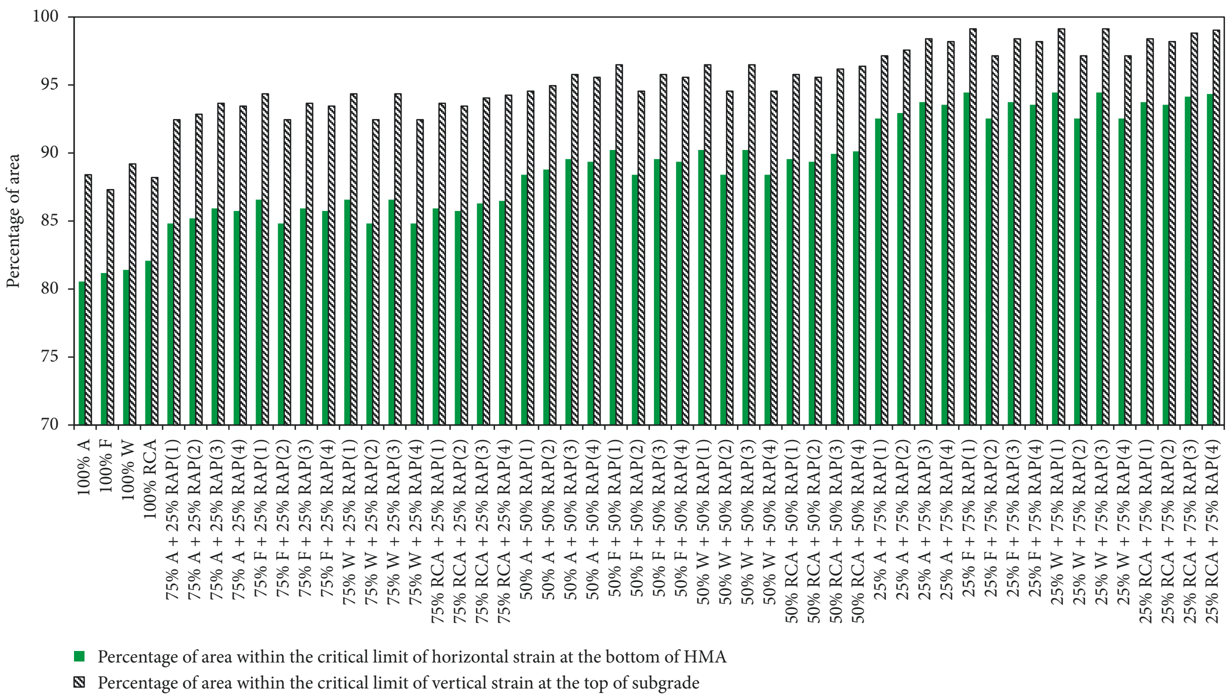

Figure 10: Percentage of area within the critical limits for horizontal strain at the bottom of HMA and vertical strain at the top of subgrade.

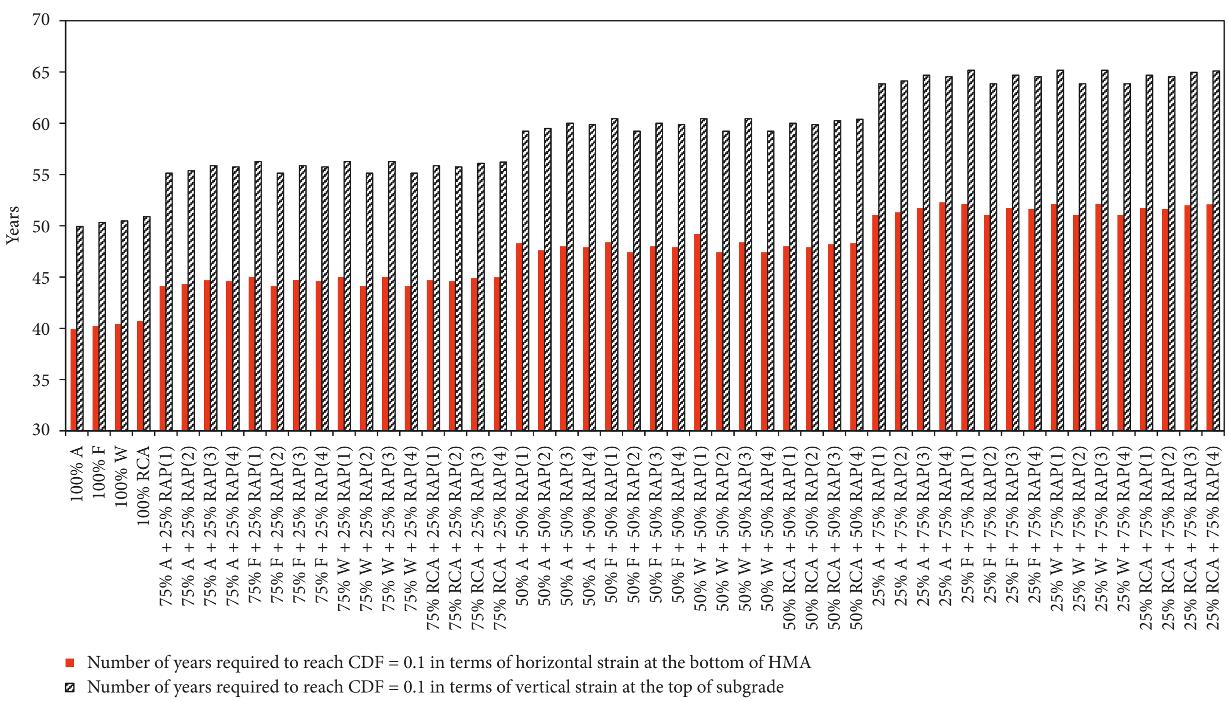

Figure 11: Number of years required to reach CDF = 0.1 in terms of horizontal strain at the bottom of HMA and vertical strain at the top of subgrade.

samples under the same loading conditions, while variations between M_R values and the applied bulk stresses during the resilient modulus tests can be approximated through power law having coefficient of correlation (r) value in the range of 0.97–0.99.

(2) The CBR values of blended samples decrease with the addition of RAP contents; however, a clear decreasing trend in conjunction with an increasing percentage of RAP contents could not be found.

(3) The new model for the estimation of M_R values includes the stress state through the experimentally determined CBR having a coefficient of correlation "r" equal to approximately 0.9, with fair distribution of the data points (M_R measured and M_R estimated) about

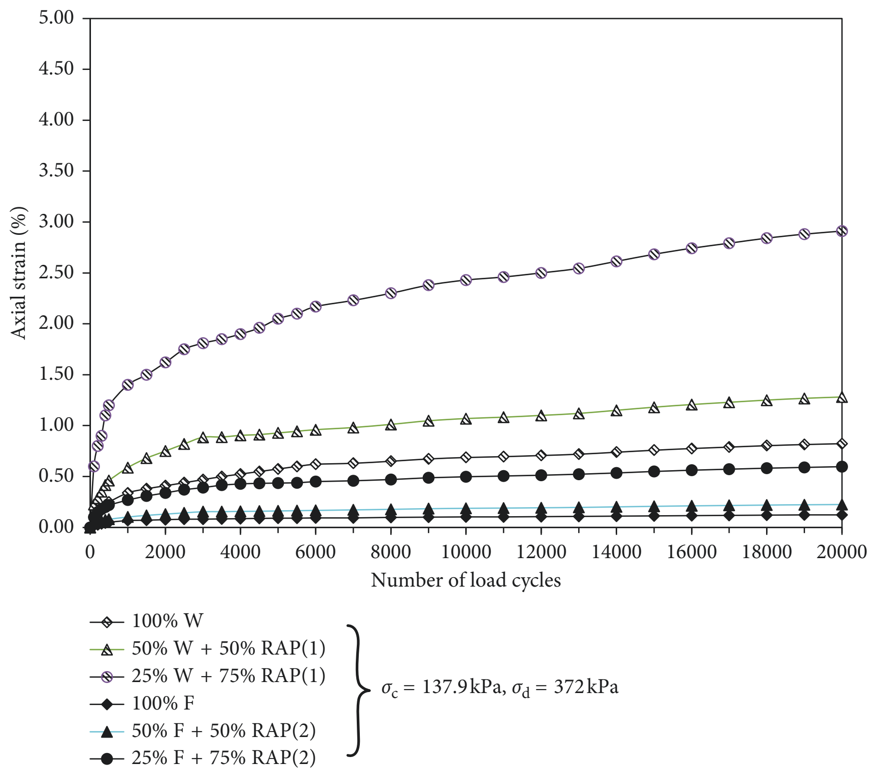

FIGURE 12: Effect of RAP contents on residual strain under long-term repeated loading.

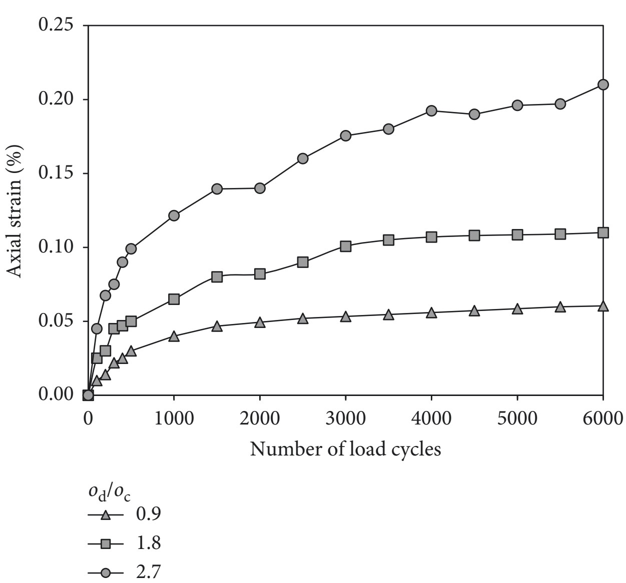

FIGURE 13: Effect of ratio of "*cyclic deviator stress to the confining stress* (σ_d/σ_c)" on the residual strain under long-term repeated loading.

the unity line indicating that the proposed regression model has a moderate to strong correlation.

(4) Statistical analysis of simulation results based on PerRoad and KenPave software demonstrates that the addition of RAP contents in the subbase layer of the flexible pavement significantly improves its performance against rutting and fatigue.

(5) Residual strain during the long-term repeated load triaxial test was found to increase in line with an increase in the ratio of "*cyclic deviator stress to the confining stress* (σ_d/σ_c)" in correlation to an increase in the percentage of RAP contents in the blended sample;

(6) From the author's perspective, the addition of RAP contents beyond a certain limit (~50%) may prove to be detrimental for the overall performance of flexible pavement structure.

Data Availability

The experimental data used to support the findings of this study are included within the article in the form of graphs and tables.

Conflicts of Interest

The author declares that there are no conflicts of interest regarding the publication of this paper.

References

[1] R. B. Mallick and A. Veeraragavan, "Sustainable pavements in India-the time to start is now," *New Building Materials and Construction World (NBM&CW) Magazine*, vol. 16, no. 3, pp. 128–140, 2010.

[2] A. Mohammadinia, A. Arulrajah, S. Horpibulsuk, and A. Chinkulkijniwat, "Effect of fly ash on properties of crushed brick and reclaimed asphalt in pavement base/subbase

applications," *Journal of Hazardous Materials*, vol. 321, pp. 547–556, 2017.

[3] L. R. Hoyos, A. J. Puppala, and C. A. Ordonez, "Characterization of cement-fiber-treated reclaimed asphalt pavement aggregates: preliminary investigation," *Journal of Materials in Civil Engineering*, vol. 23, no. 7, pp. 977–989, 2011.

[4] R. Taha, A. Al-Harthy, K. Al-Shamsi, and M. Al-Zubeidi, "Cement stabilization of reclaimed asphalt pavement aggregate for road bases and subbases," *Journal of Materials in Civil Engineering*, vol. 14, no. 3, pp. 239–245, 2002.

[5] A. M. Azam and D. A. Cameron, "Geotechnical properties of blends of recycled clay masonry and recycled concrete aggregates in unbound pavement construction," *Journal of Materials in Civil Engineering*, vol. 25, no. 6, pp. 788–798, 2013.

[6] A. Gabor and D. Cameron, "Properties of recycled concrete aggregate for unbound pavement construction," *Journal of Materials in Civil Engineering*, vol. 24, no. 6, pp. 754–764, 2012.

[7] C. S. Poon and D. Chan, "Feasible use of recycled concrete aggregates and crushed clay brick as unbound road sub-base," *Construction and Building Materials*, vol. 20, no. 8, pp. 578–585, 2006.

[8] A. Arulrajah, M. M. Y. Ali, M. M. Disfani, J. Piratheepan, and M. W. Bo, "Geotechnical performance of recycled glass-waste rock blends in footpath bases," *Journal of Materials in Civil Engineering*, vol. 25, no. 5, pp. 653–661, 2013.

[9] L. T. Lee Jr., "Recycled glass and dredged materials," Report No. ERDC TNDOER-T8, US Army Corps of Engineers, Engineer Research and Development Center, Mississippi, MS, USA, 2007.

[10] M. Ali, A. Arulrajah, M. Disfani, and J. Piratheepan, "Suitability of using recycled glass—crushed rock blends for pavement subbase applications," in *Proceedings of the Geo-Frontiers 2011 Conference on Geotechnical Foundation Design*, pp. 1325–1334, ASCE, Reston, VA, USA, 2011.

[11] J. Wartman, D. G. Grubb, and A. S. M. Nasim, "Select engineering characteristics of crushed glass," *Journal of Materials in Civil Engineering*, vol. 16, no. 6, pp. 526–539, 2004.

[12] W. Kim and J. Labuz, *Resilient Modulus and Strength of Base Course with Recycled Bituminous Material*, Minnesota Department of Transportation Research Services Section, MN, USA, 2007.

[13] D. Bloomquist, G. Diamond, M. Oden, B. Ruth, and M. Tia, *Engineering and Environmental Aspects of Recycled Materials for Highway Construction*, Appendix 1: Final Report, 1993.

[14] A. Hussain and Q. Yanjun, "Evaluation of asphalt mixes containing reclaimed asphalt pavement for wearing courses," in *Proceedings of the International Conference on Traffic and Transportation Engineering,* School of Civil Engineering, Southwest Jiaotong University, Chengdu, China, 2012.

[15] M. Solaimanian and M. Tahmoressi, "Variability analysis of hot-mix asphalt concrete containing high percentage of reclaimed asphalt pavement," *Transportation Research Record: Journal of the Transportation Research Board*, vol. 1543, no. 1, pp. 89–96, 1996.

[16] A. Gabr and D. A. Cameron, "Properties of recycled concrete aggregate for unbound pavement construction," *Journal of Materials in Civil Engineering*, vol. 24, no. 6, pp. 754–764, 2011.

[17] W.-L. Huang, D.-H. Lin, N.-B. Chang, and K.-S. Lin, "Recycling of construction and demolition waste via a mechanical sorting process," *Resources, Conservation and Recycling*, vol. 37, no. 1, pp. 23–37, 2002.

[18] A. R. Pasandín and I. Pérez, "Overview of bituminous mixtures made with recycled concrete Aggregates," *Construction and Building Materials*, vol. 74, pp. 151–161, 2015.

[19] P. Jitsangiam, H. Nikraz, and K. Siripun, "Construction and demolition (C&D) waste as a road base material for Western Australia roads," *Australian Geomechanics*, vol. 44, no. 3, pp. 57–62, 2009.

[20] A. Nataatmadja and Y. L. Tan, "Resilient response of recycled concrete road aggregates," *Journal of Transportation Engineering*, vol. 127, no. 5, pp. 450–453, 2001.

[21] C. Leek and K. Siripun, "Specification and performance of recycled materials in road pavements," Contract Rep (01119-1), 2010.

[22] J. Green and J. Hall, *Nondistructive Vibratory Testing of Airport Pavement*, 1975.

[23] W. Heukelom and A. Klomp, "Dynamic testing as a means of controlling pavements during and after construction," in *Proceedings of the International Conference on the Structural Design of Asphalt Pavements*, University of Michigan, Ann Arbor, MI, USA, 1962.

[24] Ohio Department of Transportation, *Pavement Design Manual*, Ohio Department of Transportation, Office of Pavement Engineering, OH, USA, 2008.

[25] W. D. Powell, H. C. Mayhew, and M. M. Nunn, "The structural design of bituminous roads," Laboratory Report 1132, Transport and Road Research Laboratory, Crowthorne, UK, 1984.

[26] M. W. Witczak, X. Qi, and M. W. Mirza, "Use of nonlinear subgrade modulus in AASHTO design procedure," *Journal of Transportation Engineering*, vol. 121, no. 3, 1995.

[27] AASHTO, *Guide for Design of Pavement Structures*, Washington, DC, USA, 1993.

[28] Asphalt Institute, *Research and Development of The Asphalt Institute's Thickness Design Manual (MS-1)*, 9th edition, 1982.

[29] T. Buu, *Correlation of Resistance R-value and Resilient Modulus of Idaho Subgrade Soil*, Idaho Department of Transportation, Division of Highways, ID, USA, 1980.

[30] S. Muench, J. Mahoney, and L. Pierce, *WSDOT Pavement Guide*, Washington State Department of Transportation, Internet Module, Washington, DC, USA, 2009.

[31] S. Yeh and C. Su, "Resilient properties of Colorado soils," Report No. CDOH-DH-SM-89-9, Colorado Department of Highways, Denver, CO, USA, 1989.

[32] M. R. Thompson and Q. L. Robnett, "Resilient properties of subgrade soils," *Transportation Engineering Journal of ASCE*, vol. 105, pp. 71–89, 1979.

[33] W. Lee, N. C. Bohra, A. G. Altschaeffl, and T. D. White, "Resilient modulus of cohesive soils," *Journal of Geotechnical and Geoenvironmental Engineering*, vol. 123, no. 2, pp. 131–136, 1997.

[34] R. Carmichael III and E. Stuart, "Predicting resilient modulus: a study to determine the mechanical properties of subgrade soils," *Transportation Research Record*, vol. 1043, pp. 145–148, 1986.

[35] E. C. Drumm, Y. Boateng-Poku, and T. Johnson Pierce, "Estimation of subgrade resilient modulus from standard tests," *Journal of Geotechnical Engineering*, vol. 116, no. 5, pp. 774–789, 1990.

[36] M. J. Farrar and J. P. Turner, *Resilient Modulus of Wyoming Subgrade Soils*, 1991.

[37] M. P. Jones and M. W. Witczak, "Subgrade modulus on the san diego test road," *Transportation Research Record: Journal of the Transportation Research Board*, vol. 641, pp. 1–6, 1977.

[38] A. M. Rahim and K. P. George, "Subgrade soil index properties to estimate resilient modulus," in *Proceedings of the 83th Annual Meeting of the Transportation Research Board*, National Research Council, Washington, DC, USA, 2004.

[39] M. R. Thompson and T. G. LaGrow, *A Proposed Conventional Flexible Pavement Thickness Design Procedure*, University of Illinois, Peoria, IL, USA, 1988.

[40] R. Pezo, "A general method of reporting resilient modulus tests of soils, a pavement engineer's point of view," in *Proceedings of the 72nd Annual Meeting of Transportation Research Board*, Washington, DC, USA, 1993.

[41] R. G. Hicks and C. L. Monismith, "Resilient properties of granular material," *Transportation Research Record*, vol. 345, pp. 15–31, 1971.

[42] J. Uzan, "Characterization of granular materials," *Transportation Research Record: Journal of the Transportation Research Board*, vol. 1022, pp. 52–59, 1985.

[43] National Cooperative Highway Research Program, "Guide for mechanistic-empirical design of new and rehabilitated pavement structures," NCHRP 1-37A, NCHRP, Washington, DC, USA, 2004.

[44] N. M. Louay, H. T. Hani, and H. Ananda, "Evaluation of resilient modulus of subgrade soil by cone penetration test," *Transportation Research Record: Journal of the Transportation Research Board*, vol. 1652, pp. 236–245, 1999.

[45] S. Dai and J. Zollars, "Resilient modulus of Minnesota road research project subgrade soil," *Transportation Research Record: Journal of the Transportation Research Board*, vol. 1786, no. 1, pp. 20–28, 2002.

[46] L. Mohammad, B. Huang, A. Puppala, and A. Allen, "Regression model for resilient modulus of subgrade soils," *Transportation Research Record: Journal of the Transportation Research Board*, vol. 1687, no. 1, pp. 47–54, 1999.

[47] B. Santa, "Resilient modulus of subgrade soils: comparison of two constitutive equations," *Transportation Research Record: Journal of the Transportation Research Board*, vol. 1462, pp. 79–90, 1994.

[48] H. Von Quintus and B. Killingsworth, *Analyses Relating to Pavement Material Characterizations and their Effects on Pavement Performance*, 1998.

[49] O. Porter, "The preparation of subgrades," in *Proceedings of the Nineteenth Annual Meeting Highway Research Board*, Washington, DC, USA, December 1939.

[50] O. J. Porter, "Development of the original method for highway design," *Transactions of the American Society of Civil Engineers*, vol. 115, pp. 461–467, 1950.

[51] D. W. Hight and M. G. H. Stevens, "An analysis of the California Bearing Ratio test in saturated clays," *Géotechnique*, vol. 32, no. 4, pp. 315–322, 1982.

[52] P. R. Fleming and C. D. F. Rogers, "Assessment of pavement foundations during construction," *Proceedings of the Institution of Civil Engineers-Transport*, vol. 111, no. 2, pp. 105–115, 1995.

[53] M. R. Thompson, R. Marshall, and Q. L. Robnett, "Resilient properties of subgrade soils," Final Report No. FHWA-IL-UI-160, University of Illinois, Urbana, IL, USA, 1976.

[54] B. Sukumaran, V. Kyatham, A. Shah, and D. Sheth, "Suitability of using California bearing ratio test to predict resilient modulus," in *Proceedings: Federal Aviation Administration Airport Technology Transfer Conference*, Atlantic City, NJ, USA, 2002.

[55] N. W. Lister and D. Powell, "Design practices for pavements in the United Kingdom," in *Proceedings of the 6th International Conference on the Structural Design of Asphalt Pavements*, Ann Arbor, MI, USA, July 1987.

[56] S. Hossain, G. Dickerson, and C. Weaver, *Comparative Study of VTM and AASHTO Test Method for CBR*, Co Materials Division, VDOT, 2005.

[57] N. Garg, A. Larkin, and H. Brar, "A comparative subgrade evaluation using CBR, vane shear, light weight deflectometer, and resilient modulus tests," in *Proceedings of the 8th International Conference on the Bearing Capacity of Roads, Railways and Airfields*, CRC Press, Champaign, IL, USA, 2009.

[58] M. Ayres, *Development of a rational probabilistic approach for flexible pavement analysis*, University of Maryland, College Park, MD, USA, 1997.

[59] AASHTO T. 307, *Determining the Resilient Modulus of Soils and Aggregate Materials (2012)*, American Association of State Highway and Transportation Officials, Washington, DC, USA, 2004.

[60] M. Arshad and M. F. Ahmed, "Potential use of reclaimed asphalt pavement and recycled concrete aggregate in base/subbase layers of flexible pavements," *Construction and Building Materials*, vol. 151, pp. 83–97, 2017.

[61] M. Arshad, "Correlation between resilient modulus (MR) and constrained modulus (Mc) values of granular materials," *Construction and Building Materials*, vol. 159, pp. 440–450, 2018.

[62] P. Guo and J. Emery, "Importance of strain level in evaluating resilient modulus of granular materials," *International Journal of Pavement Engineering*, vol. 12, no. 2, pp. 187–199, 2011.

[63] E. J. McGarrah, "Evaluation of current practices of reclaimed asphalt pavement/virgin aggregate as base course material," No. WA-RD 713.1, Federal Highway Administration, Washington, DC, USA, 2007.

[64] T. B. Alam, M. Abdelrahman, and S. A. Schram, "Laboratory characterisation of recycled asphalt pavement as a base layer," *International Journal of Pavement Engineering*, vol. 11, no. 2, pp. 123–131, 2010.

[65] T. Bennert and A. Maher, "The development of a performance specification for granular base and subbase material," Report No. FHWA-NJ-2005-003, Department of Transportation, Ewing Township, NJ, USA, 2005.

[66] T. H. Wonnacott, H. Thomas, and J. Ronald, "Regression: a second course in statistics," No. 04, QA278.2, W6, Wiley, New York, NY, USA, 1981.

[67] W. Penny and S. Roberts, *Neural network predictions with error bars, Dept. of Electrical and Electronic Engineering, Technology and Medicine*, Research Report TR-97-1, Imperial College of Science, London, UK, 1997.

[68] R. Dybowski and S. J. Roberts, "Confidence intervals and prediction intervals for feed-forward neural networks," *Clinical Applications of Artificial Neural Networks*, pp. 298–326, 2001.

[69] J. Hauke and T. Kossowski, "Comparison of values of Pearson's and Spearman's correlation coefficients on the same sets of data," *Quaestiones Geographicae*, vol. 30, no. 2, pp. 87–93, 2011.

[70] K.-z. Yan, H.-b. Xu, and G.-h. Shen, "Novel approach to resilient modulus using routine subgrade soil properties,"

International Journal of Geomechanics, vol. 14, no. 6, article 04014025, 2013.

[71] Y. H. Chan, "Biostatistics 104: correlational analysis," *Singapore Medical Journal*, vol. 44, no. 12, pp. 614–619, 2003.

[72] B. M. Damghani, D. Welch, C. O'Malley, and S. Knights, "The misleading value of measured correlation," *Wilmott*, vol. 2012, no. 62, pp. 64–73, 2012.

[73] L. B. Christensen, B. Johnson, and L. A. Turner, "Research methods, design, and analysis," 2011.

[74] W. J. Dixon and F. J. Massey, *Introduction to Statistical Analysis*, McGraw-Hill, New York, NY, USA, 1969.

[75] B. Colbert and Z. You, "The determination of mechanical performance of laboratory produced hot mix asphalt mixtures using controlled RAP and virgin aggregate size fractions," *Construction and Building Materials*, vol. 26, no. 1, pp. 655–662, 2012.

[76] D. H. Timm and D. E. Newcomb, "Perpetual pavement design for flexible pavements in the US," *International Journal of Pavement Engineering*, vol. 7, no. 2, pp. 111–119, 2006.

[77] Y. H. Huang, *Pavement Analysis and Design*, Prentice-Hall, Englewood Cliffs, NJ, USA, 2nd edition, 1993.

[78] L. Walubita, W. Liu, and T. Scullion, *Texas perpetual pavements-Experience overview and the way forward: Technical Report No 0-4822-3*, Texas Transportation Institute, Texas A&M University, College Station, TX, USA, 2010.

[79] D. Timm and D. Newcomb, "Calibration of flexible pavement performance equations for Minnesota road research project," *Transportation Research Record: Journal of the Transportation Research Board*, no. 1853, pp. 134–142, 2003.